

Article

Direct Utilization of Near-Infrared Light for Photooxidation with a Metal-Free Photocatalyst

Le Zeng , Zhonghe Wang, Tiexin Zhang * and Chunying Duan *

State Key Laboratory of Fine Chemicals, Dalian University of Technology, Dalian 116024, China; zengle@dlut.edu.cn (L.Z.); zhhwang@mail.dlut.edu.cn (Z.W.)

* Correspondence: zhangtiexin@dlut.edu.cn (T.Z.); cyduan@dlut.edu.cn (C.D.)

Abstract: Near-infrared (NIR) light-triggered photoredox catalysis is highly desirable because NIR light occupies almost 50% of solar energy and possesses excellent penetrating power in various media. Herein we utilize a metal-free boron dipyrromethene (BODIPY) derivative as the photocatalyst to achieve NIR light (720 nm LED)-driven oxidation of benzylamine derivatives, sulfides, and aryl boronic acids. Compared to blue light-driven photooxidation using Ru(bpy)₃Cl₂ as a photocatalyst, NIR light-driven photooxidation exhibited solvent independence and superior performance in large-volume (20 mL) reaction, presumably thanks to the neutral structure of a BODIPY photocatalyst and the deeper penetration depth of NIR light. We further demonstrate the application of this metal-free NIR photooxidation to prodrug activation and combination with Cu-catalysis for cross coupling reaction, exhibiting the potential of metal-free NIR photooxidation as a toolbox for organic synthesis and drug development.

Keywords: near-infrared light; BODIPY; photoredox catalysis; prodrug activation



Citation: Zeng, L.; Wang, Z.; Zhang, T.; Duan, C. Direct Utilization of Near-Infrared Light for Photooxidation with a Metal-Free Photocatalyst. *Molecules* **2022**, *27*, 4047. <https://doi.org/10.3390/molecules27134047>

Academic Editors: Yuanwei Zhang and Ling Huang

Received: 6 June 2022

Accepted: 22 June 2022

Published: 23 June 2022

Publisher's Note: MDPI stays neutral with regard to jurisdictional claims in published maps and institutional affiliations.



Copyright: © 2022 by the authors. Licensee MDPI, Basel, Switzerland. This article is an open access article distributed under the terms and conditions of the Creative Commons Attribution (CC BY) license (<https://creativecommons.org/licenses/by/4.0/>).

1. Introduction

In the past decades, photoredox catalysis has undergone unprecedented growth and become an important tool for organic synthesis, drug development, and polymer science [1,2]. However, the applied incident light is mainly ultraviolet or short wavelength visible light ($\lambda < 500$ nm) in the current photocatalysis setup, which leads to challenges and limitations [3,4]. For example, the short-wavelength incident light will not be exclusively absorbed by the photocatalyst in the presence of the colored reagents or reaction intermediates, leading to the formation of by-products, to low product yield, and to limited reaction scope. In addition, due to the shallow penetration of short wavelength light in various reaction media [5], the scale-up of visible light-driven photocatalysis suffers from slow reaction rates and decreased reaction yields, which is detrimental to industrial application.

In this context, utilizing a longer-wavelength light, in particular near-infrared (NIR, $\lambda > 650$ nm) light, as an energy source for photocatalysis emerged as a hot topic since it can obviate the above-mentioned limitations [5–7]. Compared to visible light, NIR light exhibits higher penetration depth in various media with weak scattering and diffuse reflection, especially for biological tissue, thus benefiting the effective light absorption by a photocatalyst in scale-up reactions [5,8,9]. The weaker energy of NIR light compared to visible light can circumvent light-induced degradation of the photocatalyst and substrates, thus enabling lower catalyst loading and better reaction selectivity [5,8,9]. In addition, the nearly 50% occupancy of NIR in solar energy provides a clean and infinite source of NIR light [8]. Despite these obvious advantages, NIR light-driven photoredox catalysis was rarely reported [8–10], largely due to the poor absorption of NIR light for conventional photocatalysts [3,4]. Currently there are two different approaches to achieve NIR photoredox catalysis. One is the indirect utilization of NIR light via an up-conversion strategy that converts NIR light to high-energy visible light; for example, the triplet-triplet

annihilation up-conversion (TTA-UC) strategy [11,12]. Normally, the photoactivation procedure of TTA-UC-mediated NIR photoredox catalysis requires the involvement of multiple energy transfer steps between the sensitizer, annihilator, and visible light photocatalyst [11]. Obviously, the complexity makes this indirect approach not easy to handle. On the other hand, the direct utilization of NIR for photoredox catalysis relies on the use of a noble metal-based photocatalyst, which is expensive and might lead to toxic heavy-metal residue for the product [8,9]. Thus, direct NIR photoredox catalysis with a metal-free photocatalyst is a long-term goal in solar energy use. Notably, in the preparation of this paper, cyanines were reported to conduct NIR organic photoredox catalysis, constituting the only one example of metal-free NIR photoredox catalyst [13].

In other hand, iodinated BODIPY derivatives are well-known as metal-free photocatalysts for visible-light photoredox catalysis because of their strong light absorption ability (molar extinction coefficient of 10^5 or more), high triplet quantum yield (>90%), long triplet excited state lifetime (>2 μ s), robust photostability, and easily tailorable structure [14,15]. However, there are no reports of NIR-activated BODIPY as photocatalysts. Recently, carbazole-substituted iodinated BODIPY (BDP) was utilized as an efficient photosensitizer for ultralow-power NIR-triggered photodynamic therapy thanks to its intense absorption in the NIR region and its remarkably high singlet oxygen quantum yield (67%) [16]. Considering the iodinated BODIPY core and the solubility-improving long chain of BDP, we anticipated that BDP can be applied as an efficient metal-free photocatalyst via direct NIR light utilization.

Herein we report the successful utilization of NIR light (720 nm LED) as the energy source for BDP-catalyzed photooxidation (Figure 1). After being excited by NIR light, BDP undergoes the intersystem crossing (ISC) process to reach its triplet-excited state ($^3\text{BDP}^*$); this in turn can transfer energy to oxygen, forming the singlet oxygen ($^1\text{O}_2$), or conduct electron transfer process to finally generate the superoxide anion ($\text{O}_2^{\bullet-}$). These generated reactive oxygen species are the terminal oxidant to achieve efficient oxidation of benzylamine derivatives, sulfides, and aryl boric acids. Notably, compared to the state-of-art blue-light photocatalyst $\text{Ru}(\text{bpy})_3\text{Cl}_2$, this NIR photocatalyst BDP exhibits solvent independence and better scalability in photooxidation, possibly benefiting from the neutral molecular structure and penetration power of NIR light. Furthermore, we demonstrate the wide applicability of NIR-driven photooxidation with BDP through aryl boric acid-involving prodrug activation as well as the combination with Cu catalysis for carbon-carbon cross coupling.

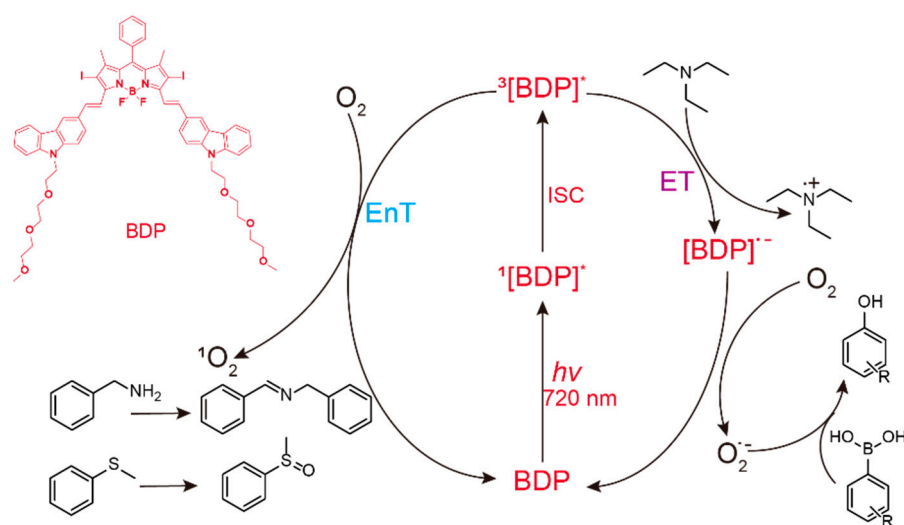


Figure 1. Mechanism of NIR-driven BDP-catalyzed photooxidation.

2. Results and Discussion

BDP was synthesized according to the reported procedure [16], and the photophysical properties of BDP were investigated in dichloromethane (DCM). As shown in Figure S1, the absorption peak of BDP located at 709 nm with a high molar extinction coefficient ($9.5 \times 10^4 \text{ M}^{-1}\text{cm}^{-1}$). In addition, no obvious photobleaching of BDP was detected after 3 h of NIR illumination (720 nm LED, 20 mW/cm²) (Figure S2), verifying its robust photostability. The fluorescence emission peak of BDP located at 750 nm with a quantum yield as low as 4% since the heavy atom effect of iodine promoted the transition from ¹BDP* to ³BDP* [15,16]. Importantly, the singlet oxygen quantum yield of BDP was measured to be 65% at 710 nm using the established method [15].

In view of the high ¹O₂ production efficiency of BDP, BDP was then used as the photocatalyst for the benzylamine coupling reaction under NIR light illumination. The photooxidation coupling of benzylamine with ¹O₂ as the terminal oxidant was an important probe reaction to afford Schiff bases [17–20], which are useful building blocks in the synthesis of fine chemicals, functional materials, and useful drugs [21–23]. Conventional photocatalysts such as g-C₃N₄, TiO₂, Ir(ppy)₃, and [Ru(bpy)₃]²⁺ were all applied in the photooxidation of benzylamine (**1a**), utilizing visible light or UV as the excitation source [17–20]. With extra-low BDP loading (~0.06 mol%) and mild NIR irradiation (720 nm, 20 mW/cm²), the quantitative conversion of benzylamine to a Schiff base (**2a**) was observed after 2 h reaction in DCM (See Table S1 for detailed reaction setup). No product was detectable in the absence of light, BDP, or oxygen, indicating that NIR illumination, BDP, and oxygen were all required for this reaction to proceed (Table S1). Additionally, the effect of solvent polarity on this NIR-driven BDP-catalyzed benzylamine coupling was explored. High conversions of benzylamine were obtained with various solvents such as acetonitrile (CH₃CN, a highly polar aprotic solvent), methanol (MeOH, a highly polar protic solvent), and the medium polar solvents DCM and ethyl acetate (EtOAc), suggesting that the polarity of the solvent has an insignificant effect on BDP-catalyzed NIR-driven photocatalysis (Table S1). By contrast, Ru(bpy)₃Cl₂ exhibited strong dependence of the solvent for benzylamine photooxidation. In CH₃CN, Ru(bpy)₃Cl₂ enabled the formation of a Schiff base with a conversion of 100% whereas only 5% conversion was obtained in DCM (Figure S3). This solvent dependence of Ru(bpy)₃Cl₂ may result from the sensitivity of the chloride counter-anion [24], which in turn reflected the robustness of the organic-neutral NIR photocatalyst, BDP.

The scale-up photooxidation of benzylamine with the combination of BDP and NIR light or Ru(bpy)₃Cl₂ and blue light was then explored. The amounts of the substrate benzylamine and photocatalysts were enlarged by 20 times for a 20 mL reaction. As shown in Figure 2, Ru(bpy)₃Cl₂ gave a sharp decline in conversion rate from 100% at 1 mL to 38% at 20 mL. In sharp contrast, the high conversion rate of 88% was still achieved with BDP as photocatalyst under NIR irradiation in 20 mL reaction. This result clearly demonstrated that NIR light can penetrate deeper into a reaction solution than visible light, and thus NIR-triggered photoredox catalysis is more suitable and efficient for large-scale or industrial application.

To explore the substrate scope of this NIR light-driven BDP-catalyzed aerobic oxidation, a variety of benzylamine derivatives were investigated. Electron-rich amines such as 4-methoxybenzylamine (Table 1, entry 2, **2b**) and electron-deficient amines substituted by halogens or trifluoromethyl groups (Table 1, entries 3–7) were all efficiently converted to the corresponding Schiff base, indicating that the electronic nature of substrates does not impact NIR-driven photooxidation. The nearly identical photoconversion rates of *ortho*- (**1d**), *meta*- (**1e**), and *para*-chloro (**1c**)-substituted benzylamines demonstrated that the position of the substituents had little impact on this NIR-driven BDP-catalysis (Table 1, entries 3–5). Moreover, the good conversion (77%) of benzylamine with steric hindrance (Table 1, entry 8) showed that steric hindrance cannot inhibit efficient photocoupling. Secondary amine substrates such as tetrahydroisoquinoline and dibenzylamine can also be transformed to the corresponding Schiff base by a BDP photocatalyst with a conversion of 59% and 100%, respectively (Table 1, entries 9–10). The above experimental results verified

that BDP was an excellent NIR photocatalyst to efficiently promote the oxidative coupling of benzylamine derivatives with broad substrate scope.

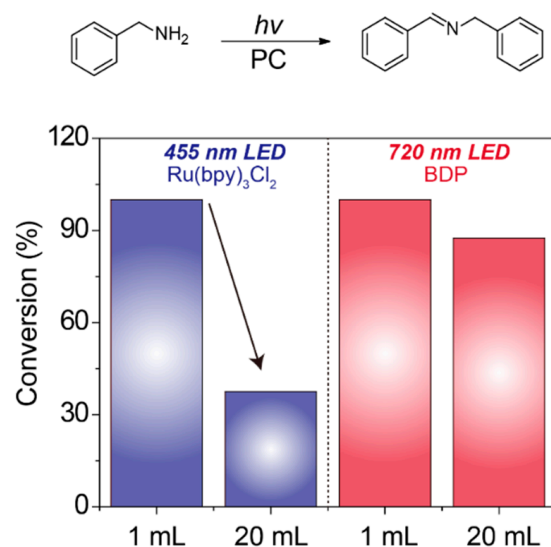


Figure 2. Comparative photocatalytic performance of Ru(bpy)₃Cl₂ and BDP for benzylamine coupling in different reaction volumes.

Table 1. Oxidation of various amines using BDP as the photocatalyst under NIR illumination ^a.

Entry	Substrate	Product	Conversion ^b	TON ^c	TOF (min ⁻¹) ^d
1			100	8.59 × 10 ²	7.16
2			100	8.59 × 10 ²	7.16
3			95.6	8.22 × 10 ²	6.85
4			95.2	8.18 × 10 ²	6.82
5			100	8.59 × 10 ²	7.16
6			100	8.59 × 10 ²	7.16
7			100	8.59 × 10 ²	7.16
8 ^e			76.9	6.61 × 10 ²	5.51
9			58.8	5.05 × 10 ²	4.21
10			100	8.59 × 10 ²	7.16

^a Reaction conditions: amine (0.275 mmol), BDP (1.6 × 10⁻⁴ mmol, 0.2 mg), DCM (1 mL), 720 nm LED (20 mW/cm²), under air atmosphere, 2 h, room temperature. ^b Conversion determined by ¹H NMR. ^c Turnover number (TON) value was calculated as mole of amine converted per mol of BDP. ^d Turnover frequency (TOF) was equal to TON divided by irradiation time. ^e In methanol.

The mechanism investigation of this NIR-driven BDP-catalyzed benzylamine coupling was then performed. In the presence of a singlet oxygen quencher (triethylenediamine, DABCO) [25], the generation of the Schiff base was negligible, indicating that singlet oxygen played an important role in this photoredox catalysis (Table S2). In contrast, a good isolated yield of 84% was still obtained after adding high concentration of benzoquinone (BQ) [25], the trapping agent of superoxide anion, which ruled out the dominative role of superoxide

anion in this NIR-photocatalytic system. In addition, the reaction rate in deuterated chloroform (CDCl_3) was nearly twice that in DCM (Table S2). Since deuterated solvents were reported to stabilize $^1\text{O}_2$ [26], this enhanced reaction rate in CDCl_3 further supported the assumption that $^1\text{O}_2$ was the key species for this BDP-catalyzed NIR photooxidation. To confirm this proposal, the $^1\text{O}_2$ generation in the presence of BDP was measured by using 1,3-diphenylbenzofuran (DPBF) as the $^1\text{O}_2$ indicator [15]. Under the irradiation of NIR light (720 nm, 5 mW/cm²), the absorption of DPBF was significantly reduced in the presence of BDP (Figure S4), suggesting that BDP could trigger the generation of $^1\text{O}_2$ with NIR light irradiation. Combined with the above experimental results, the proposed mechanism of this BDP-catalyzed NIR-driven oxidation of amines was outlined (Figure S5). BDP was firstly excited by NIR light to reach its singlet excited state ($^1[\text{BDP}]^*$); then it underwent the intersystem crossing (ISC) process to generate the triplet excited state $^3[\text{BDP}]^*$ [15]. Singlet oxygen ($^1\text{O}_2$) was generated via triplet–triplet energy transfer from $^3[\text{BDP}]^*$ to molecular oxygen. The substrate benzylamine was firstly oxidized by $^1\text{O}_2$ to produce hydrogen peroxide and the intermediate imine, which further condensed with the second molecule of benzylamine to yield the final product, the Schiff base.

As shown in Figure 3, this NIR photooxidation of benzylamine could be further combined with copper catalysis (using copper trifluoroacetate, $\text{Cu}(\text{OTf})_2$, as catalyst), where the Schiff base **2a**, the in situ generated product of NIR photocatalysis, reacted with 4-*tert*-butylphenylacetylene in toluene to give an alkyne-substituted secondary amine with an isolated yield of 80% [27]. This result demonstrated that NIR light-driven photocatalysis can be merged with other catalytic systems in a tandem manner to access sophisticated functional scaffolds [28].

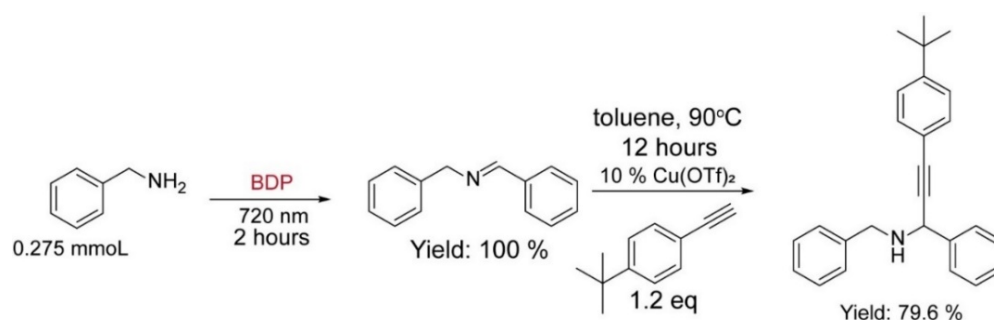
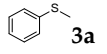
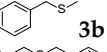
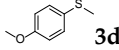
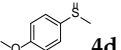


Figure 3. The tandem synthesis of the alkyne-substituted secondary amine via the combination of NIR light-driven BDP photocatalysis with copper catalysis.

Besides the photooxidation of benzylamine, the photooxidation of sulfides via the $^1\text{O}_2$ pathway was also of fundamental importance since the targeted sulfoxide motifs existed widely in organic intermediates, pharmaceutical molecules, and organic semiconductors [29–32]. BDP was then applied to NIR light-driven photooxidation of sulfides in view of its excellent singlet oxygen generation ability upon NIR light. As shown in Table 2, different sulfide derivatives, such as thioanisole (**3a**), benzyl methyl sulfide (**3b**), dibenzyl sulfide (**3c**), and 4-methoxyphenyl methyl sulfide (**3d**), were all smoothly oxidized to the corresponding sulfoxide with nearly quantitative conversions. A control experiment in the presence of DABCO led to inferior performance (11% yield), reflecting the dominative role of $^1\text{O}_2$. This result further verified that BDP was an efficient NIR photocatalyst that can generate $^1\text{O}_2$ as the terminal oxidant upon NIR light irradiation [33].

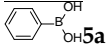
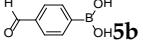
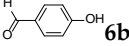
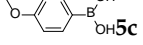
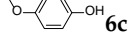
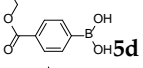
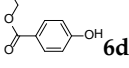
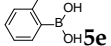
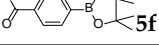
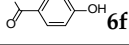
Table 2. Oxidation of various sulfides using BDP as the photocatalyst under NIR illumination ^a.

Entry	Substrate	Product	Conversion ^b	TON ^c	TOF (min ⁻¹) ^d
1			100	430	3.6
2			100	430	3.6
3			96	413	3.5
4			90	387	3.2

^a Reaction condition: sulfide (0.20 mmol), BDP (1.6×10^{-4} mmol, 0.2 mg), DCM/methanol ($v/v = 1/1$, 2 mL), 720 nm LED (20 mW/cm²), in air, 4 h, room temperature. ^b Conversion was determined by ¹H NMR. ^c TON value was calculated as mole of sulfide converted per mol of BDP. ^d TOF means turnover frequency, which equates to TON divided by irradiation time.

The triplet excited state of the photosensitizer was not only capable of sensitizing other molecules through an energy transfer pathway but can also participate in an electron transfer process to activate a substrate [15]. To test the feasibility of NIR-initiated ³BDP* in the electron transfer process, the aerobic oxidation of aryl boronic acids (**5a–5f**) was employed as the probe reaction (Table 3) [34,35]. The reactions were completed within 4 h to give the formation of corresponding substituted phenols, with satisfactory yields of 85–95%. Compared to the visible light catalytic system using Ru(bpy)₃Cl₂, the BDP-involved NIR photocatalysis furnished this reaction within much shorter time scopes [34]. Through comparative studies (Table S3), we confirmed that BDP, the electron donor triethylamine (TEA), photoirradiation, and oxygen were all indispensable for this photocatalytic oxidation. In addition, in the presence of benzoquinone (quencher of O₂^{•-}), the yield of the product dramatically dropped from 90% to less than 10%, which implied the key oxidant role of O₂^{•-} in the oxidation of boronic acids, showcasing the capability of this BDP-driven NIR photocatalysis in electron transfer-involved applications [25].

Table 3. Oxidation of various phenylboronic acid derivatives using BDP as the photocatalyst under NIR illumination ^a.

Entry	Substrate	Product	Yield ^b	TON ^c	TOF (min ⁻¹) ^d
1			85	365	3.1
2			95	408	3.4
3			90	387	3.2
4			87	374	3.1
5			94	404	3.4
6			95	408	3.4

^a Reaction condition: phenylboronic acid derivatives (0.20 mmol), triethylamine (TEA) (50 μL), BDP (1.6×10^{-4} mmol, 0.2 mg), DCM/methanol ($v/v = 1/1$, 2 mL), 720 nm LED (20 mW/cm²), in air, 4 h, room temperature. ^b Isolated yield. ^c TON value was calculated as mole of phenylboronic acid converted per mol of BDP. ^d TOF means turnover frequency, which equates to TON divided by irradiation time.

Utilizing the successful photooxidation of aryl boronic acid, we further explored the NIR-irradiated deprotection of prodrug in the presence of BDP. In comparison to the established deprotection approaches with acid/base-sensitive or redox-sensitive agents, the photolytic activation of prodrug emerged as a traceless and green alternative to allow deprotection under light illumination [36,37]. In the presence of BDP and NIR irradiation,

arylborate moieties, the protecting groups of carboxylate drugs, were firstly oxidized to phenols, which then underwent photolysis to release the corresponding pharmaceutical scaffolds such as Naproxen (**8a**) and Indomethacin (**8b**), in the yields of 74% and 67%, respectively (Figure 4) [38–40]. These results revealed the potential of our NIR light-driven photolytic deprotection strategy in a wide array of applications related to the synthesis of functional photocaged small molecules [41,42].

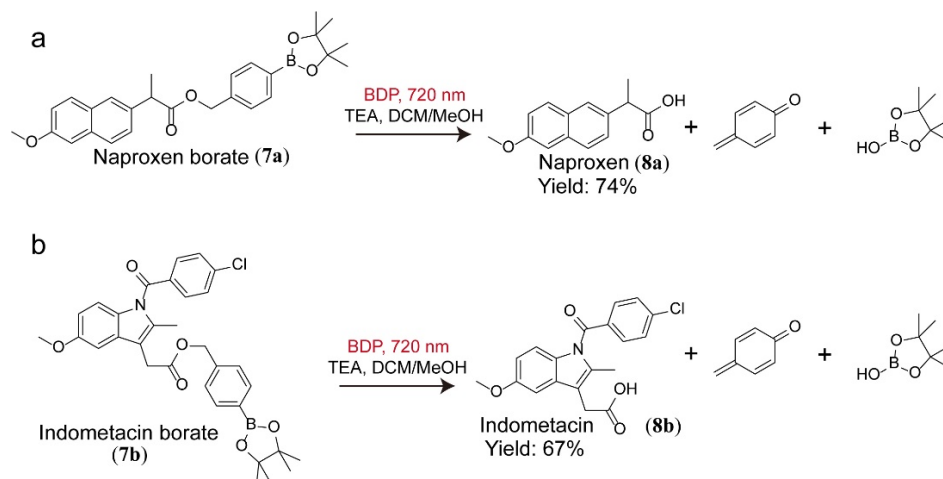


Figure 4. NIR light-driven photolytic activation of the prodrug naproxen borate (a) and indometacin borate (b) with BDP as the photocatalyst.

3. Materials and Methods

3.1. Measurement of Singlet Oxygen Generation Using DPBF as the Indicator

The mixture of BDP (10 μM) and DPBF, of which the concentration was set to make the absorbance at 414 nm to be 1.0, was irradiated with 720 nm LED (5.0 mW/cm^2). The absorption of the obtained solution was monitored every 20 s. The decrease in absorbance intensity of DPBF at 414 nm suggested that singlet oxygen was generated.

3.2. Photooxidation of Benzylamine Catalyzed by BDP with NIR Light Illumination

The mixture of benzylamine (0.275 mmol, 30 μL), BDP (1.6×10^{-4} mmol, 0.2 mg) in 1 mL dichloromethane was irradiated by 720 nm LED (20 mW/cm^2). After the reaction, the solvent was removed under reduced pressure. Then 0.6 mL deuterated chloroform was added for the measurement of conversion via ^1H NMR. For the benzylamine ($\text{NH}_2\text{-CH}_2$), the characteristic proton chemical shift located at 3.82 ppm; meanwhile, the unique chemical shift of the Schiff base product ($\text{CH}_2\text{-N=CH}$) located at 4.82 ppm. Based on the integrated area of these two peaks, the product conversion can be calculated.

3.3. The Setup of the Large-Scale Reactions

For the large-scale reaction under NIR light and blue light, the reactions were operated with a 25 mL vial under light irradiation of 20 mW/cm^2 . The mixture of benzylamine (5.5 mmol, 600 μL) and BDP (3.2×10^{-3} mmol, 4.0 mg) in 20 mL dichloromethane was irradiated by NIR light of 720 nm under air atmosphere. Meanwhile, the mixture of benzylamine (5.5 mmol, 600 μL) and $\text{Ru}(\text{bpy})_3\text{Cl}_2 \cdot 6\text{H}_2\text{O}$ (3.2×10^{-3} mmol, 2.4 mg) in 20 mL acetonitrile was irradiated by blue light of 455 nm. After the reaction, the solvent was removed under reduced pressure. Then 0.6 mL deuterated chloroform was added for the measurement of conversion via ^1H NMR. For the benzylamine ($\text{NH}_2\text{-CH}_2$), the characteristic proton chemical shift was located at 3.82 ppm, and the unique chemical shift of the Schiff base product ($\text{CH}_2\text{-N=CH}$) was located at 4.82 ppm. Based on the integrated area of these two peaks, the product conversion can be calculated.

3.4. Photooxidation of Sulfides Catalyzed by BDP with NIR-Light Illumination

The mixture of sulfides (0.20 mmol) and BDP (1.6×10^{-4} mmol, 0.2 mg) in 2 mL DCM/methanol ($v/v = 1/1$) was irradiated by 720 nm LED (20 mW/cm²) under air atmosphere. After the reaction, the solvent was removed under reduced pressure. Then 0.6 mL deuterated chloroform was added for the measurement of conversion via ¹H NMR. For the sulfide (S-CH₂ or S-CH₃), the characteristic proton chemical shift was located near 2.40 ppm, while the unique chemical shift of the sulfoxide product (CH₂-S=O or CH₃-S=O) was located near 2.72 ppm. Based on the integrated area of these two peaks, the conversion can be calculated.

3.5. Photooxidation of Phenylboronic Acids Catalyzed by BDP with NIR-Light Illumination

The mixture of phenylboronic acids (0.20 mmol), triethylamine (TEA) (50 μL), and BDP (1.6×10^{-4} mmol, 0.2 mg) in 2 mL DCM/methanol ($v/v = 1/1$) was irradiated by 720 nm LED (20 mW/cm²) under air atmosphere. After the reaction, water was added. The aqueous mixture was then extracted with ethyl acetate (EtOAc) following which the ethyl acetate layer was dried with anhydrous Na₂SO₄ and concentrated. This was followed by column chromatography over silica gel to yield the product eluent EtOAc/hexane = 3/1, v/v .

3.6. Turnover Number (TON) and Turnover Frequency (TOF) Calculation

Based on the ¹H NMR data, the conversion of the substrate can be calculated and then the amount of the product can be determined.

$$\text{TON} = \text{mole of product per mole of catalyst} \quad (1)$$

$$\text{TOF} = \text{TON/irradiation time (min)} \quad (2)$$

3.7. Tandem Reaction Catalyzed by BDP and Copper Salt

After two hours reaction of benzylamine (0.825 mmol) in the presence of the BDP (4.8×10^{-4} mmol) and 720 nm light illumination (20 mW/cm²) under air atmosphere, the solvent was removed under a vacuum. Then the reaction mixture containing imine product, a toluene solution containing 4.1×10^{-2} mmol Cu(OTf)₂, 4.1×10^{-2} mmol Na₂SO₄ (10 mol%), and 100 μL 4-tert-butylphenylacetylene, was transferred to a dried Schleck tube under nitrogen atmosphere. After reacting at 90 °C overnight, the final product of this tandem reaction was isolated by flash column chromatography on silica gel with a mixed eluent of hexane and ethyl acetate (10:1, v/v). ¹H NMR (500 MHz, CDCl₃): δ = 8.36 (s, 1H), 7.78–7.76 (m, 2H), 7.43–7.39 (m, 5H), 7.32–7.29 (m, 5H), 7.24–7.22 (m, 1H), 4.81 (s, 2H), 3.01 (s, 1H), 1.29 (s, 9H).

4. Conclusions

In summary, we employed a metal-free BODIPY-derivative, BDP, as the NIR light photocatalyst to achieve the efficient oxidation of benzylamine derivatives, sulfides, and aryl boronic acids to yield chemicals with synthetic importance and added value. The strong absorption of NIR light of BDP enabled the direct utilization of low-power NIR irradiation (720 nm LED, 20 mW/cm²) for photooxidation, which exhibited deeper penetration depth and higher efficiency in large-volume reactions than the established visible-light photocatalytic protocols. Mechanism investigation showed that BDP can effectively produce singlet oxygen via energy transfer or generate superoxide anion via electron transfer upon NIR illumination. More importantly, BDP-triggered NIR photooxidation can be further combined with Cu catalysis to yield alkyne-substituted secondary amine derivatives, or applied in photolytic prodrug activation of Naproxen-borate and Indomethacin-borate, demonstrating the infinite potential of NIR photocatalysis in sophisticated organic synthesis. This work showcased the capability of utilizing NIR light by organic dyes to forge value-added chemicals, which will benefit the development of organic synthesis, material design, and solar energy use.

Supplementary Materials: The following supporting information can be downloaded at: <https://www.mdpi.com/article/10.3390/molecules27134047/s1>, Materials and Characterization, Tables S1 to S3, Figures S1 to S5, and NMR Data of the Products [27,43–51], Figures S6–S18.

Author Contributions: Conceptualization, T.Z. and C.D.; methodology, L.Z. and Z.W.; validation, L.Z., Z.W., T.Z. and C.D.; formal analysis, L.Z., T.Z. and C.D.; investigation, L.Z. and Z.W.; resources, T.Z. and C.D.; data curation, L.Z. and Z.W.; writing—original draft preparation, L.Z. and T.Z.; writing—review and editing, C.D.; supervision, C.D.; project administration, T.Z. and C.D.; funding acquisition, L.Z., T.Z. and C.D. All authors have read and agreed to the published version of the manuscript.

Funding: This work was supported by the National Natural Science Foundation of China (Nos. 21901033, 21971031, 21820102001, 21890381) and the China Postdoctoral Science Foundation (No. 2019M651105).

Institutional Review Board Statement: Not applicable.

Informed Consent Statement: Not applicable.

Data Availability Statement: Not applicable.

Acknowledgments: We thank Ling Huang of Nankai University and Gang Han of UMass Chan Medical School for help in preparing the BDP photocatalyst.

Conflicts of Interest: The authors declare no conflict of interest.

Sample Availability: Samples of the compounds (BDP) are available from the authors.

References

1. Ravelli, D.; Dondi, D.; Fagnoni, M.; Albini, A. Photocatalysis. A multi-faceted concept for green chemistry. *Chem. Soc. Rev.* **2009**, *38*, 1999. [[CrossRef](#)] [[PubMed](#)]
2. Corrigan, N.; Shanmugam, S.; Xu, J.; Boyer, C. Photocatalysis in organic and polymer synthesis. *Chem. Soc. Rev.* **2016**, *45*, 6165–6212. [[CrossRef](#)] [[PubMed](#)]
3. Romero, N.A.; Nicewicz, D.A. Organic Photoredox Catalysis. *Chem. Rev.* **2016**, *116*, 10075–10166. [[CrossRef](#)] [[PubMed](#)]
4. Prier, C.K.; Rankic, D.A.; MacMillan, D.W.C. Visible Light Photoredox Catalysis with Transition Metal Complexes: Applications in Organic Synthesis. *Chem. Rev.* **2013**, *113*, 5322–5363. [[CrossRef](#)] [[PubMed](#)]
5. Szaciłowski, K.; Macyk, W.; Drzewiecka-Matuszek, A.; Brindell, M.; Stochel, G. Bioinorganic Photochemistry: Frontiers and Mechanisms. *Chem. Rev.* **2005**, *105*, 2647–2694. [[CrossRef](#)] [[PubMed](#)]
6. Rao, M.; Kanagaraj, K.; Fan, C.; Ji, J.; Xiao, C.; Wei, X.; Wu, W.; Yang, C. Photocatalytic Supramolecular Enantiodifferentiating Dimerization of 2-Anthracenecarboxylic Acid through Triplet–Triplet Annihilation. *Org. Lett.* **2018**, *20*, 1680–1683. [[CrossRef](#)]
7. Rao, M.; Fan, C.; Ji, J.; Liang, W.; Wei, L.; Zhang, D.; Yan, Z.; Wu, W.; Yang, C. Catalytic Chiral Photochemistry Sensitized by Chiral Hosts-Grafted Upconverted Nanoparticles. *ACS Appl. Mater. Interfaces* **2022**, *14*, 21453–21460. [[CrossRef](#)] [[PubMed](#)]
8. Ravetz, B.D.; Pun, A.B.; Churchill, E.M.; Congreve, D.N.; Rovis, T.; Campos, L.M. Photoredox catalysis using infrared light via triplet fusion upconversion. *Nature* **2019**, *565*, 343–346. [[CrossRef](#)]
9. Ravetz, B.D.; Tay, N.E.S.; Joe, C.L.; Sezen-Edmonds, M.; Schmidt, M.A.; Tan, Y.; Janey, J.M.; Eastgate, M.D.; Rovis, T. Development of a Platform for Near-Infrared Photoredox Catalysis. *ACS Cent. Sci.* **2020**, *6*, 2053–2059. [[CrossRef](#)]
10. Sellet, N.; Cormier, M.; Goddard, J.-P. The dark side of photocatalysis: Near-infrared photoredox catalysis for organic synthesis. *Org. Chem. Front.* **2021**, *8*, 6783–6790. [[CrossRef](#)]
11. Singh-Rachford, T.N.; Castellano, F.N. Photon upconversion based on sensitized triplet–triplet annihilation. *Coord. Chem. Rev.* **2010**, *254*, 2560–2573. [[CrossRef](#)]
12. Zhou, J.; Liu, Q.; Feng, W.; Sun, Y.; Li, F. Upconversion Luminescent Materials: Advances and Applications. *Chem. Rev.* **2015**, *115*, 395–465. [[CrossRef](#)] [[PubMed](#)]
13. Obah Kosso, A.R.; Sellet, N.; Baralle, A.; Cormier, M.; Goddard, J.-P. Cyanine-based near infra-red organic photoredox catalysis. *Chem. Sci.* **2021**, *12*, 6964–6968. [[CrossRef](#)] [[PubMed](#)]
14. Loudet, A.; Burgess, K. BODIPY Dyes and Their Derivatives: Syntheses and Spectroscopic Properties. *Chem. Rev.* **2007**, *107*, 4891–4932. [[CrossRef](#)]
15. Zhao, J.; Xu, K.; Yang, W.; Wang, Z.; Zhong, F. The triplet excited state of Bodipy: Formation, modulation and application. *Chem. Soc. Rev.* **2015**, *44*, 8904–8939. [[CrossRef](#)]
16. Huang, L.; Li, Z.; Zhao, Y.; Zhang, Y.; Wu, S.; Zhao, J.; Han, G. Ultralow-Power Near Infrared Lamp Light Operable Targeted Organic Nanoparticle Photodynamic Therapy. *J. Am. Chem. Soc.* **2016**, *138*, 14586–14591. [[CrossRef](#)]
17. Su, F.; Mathew, S.C.; Möhlmann, L.; Antonietti, M.; Wang, X.; Blechert, S. Aerobic Oxidative Coupling of Amines by Carbon Nitride Photocatalysis with Visible Light. *Angew. Chem. Int. Ed.* **2011**, *50*, 657–660. [[CrossRef](#)]

18. Lang, X.; Ji, H.; Chen, C.; Ma, W.; Zhao, J. Selective Formation of Imines by Aerobic Photocatalytic Oxidation of Amines on TiO₂. *Angew. Chem. Int. Ed.* **2011**, *50*, 3934–3937. [[CrossRef](#)]
19. Rueping, M.; Vila, C.; Szadkowska, A.; Koenigs, R.M.; Fronert, J. Photoredox Catalysis as an Efficient Tool for the Aerobic Oxidation of Amines and Alcohols: Bioinspired Demethylations and Condensations. *ACS Catal.* **2012**, *2*, 2810–2815. [[CrossRef](#)]
20. Beatty, J.W.; Stephenson, C.R.J. Amine Functionalization via Oxidative Photoredox Catalysis: Methodology Development and Complex Molecule Synthesis. *Acc. Chem. Res.* **2015**, *48*, 1474–1484. [[CrossRef](#)]
21. Cozzi, P.G. Metal–Salen Schiff base complexes in catalysis: Practical aspects. *Chem. Soc. Rev.* **2004**, *33*, 410–421. [[CrossRef](#)] [[PubMed](#)]
22. Jia, Y.; Li, J. Molecular Assembly of Schiff Base Interactions: Construction and Application. *Chem. Rev.* **2015**, *115*, 1597–1621. [[CrossRef](#)] [[PubMed](#)]
23. Segura, J.L.; Mancheño, M.J.; Zamora, F. Covalent organic frameworks based on Schiff-base chemistry: Synthesis, properties and potential applications. *Chem. Soc. Rev.* **2016**, *45*, 5635–5671. [[CrossRef](#)] [[PubMed](#)]
24. Farney, E.P.; Chapman, S.J.; Swords, W.B.; Torelli, M.D.; Hamers, R.J.; Yoon, T.P. Discovery and Elucidation of Counteranion Dependence in Photoredox Catalysis. *J. Am. Chem. Soc.* **2019**, *141*, 6385–6391. [[CrossRef](#)]
25. Nosaka, Y.; Nosaka, A.Y. Generation and Detection of Reactive Oxygen Species in Photocatalysis. *Chem. Rev.* **2017**, *117*, 11302–11336. [[CrossRef](#)] [[PubMed](#)]
26. Merkel, P.B.; Nilsson, R.; Kearns, D.R. Deuterium effects on singlet oxygen lifetimes in solutions. New test of singlet oxygen reactions. *J. Am. Chem. Soc.* **1972**, *94*, 1030–1031. [[CrossRef](#)]
27. Meyet, C.E.; Pierce, C.J.; Larsen, C.H. A Single Cu(II) Catalyst for the Three-Component Coupling of Diverse Nitrogen Sources with Aldehydes and Alkynes. *Org. Lett.* **2012**, *14*, 964–967. [[CrossRef](#)]
28. Lang, X.; Zhao, J.; Chen, X. Cooperative photoredox catalysis. *Chem. Soc. Rev.* **2016**, *45*, 3026–3038. [[CrossRef](#)]
29. Carreno, M.C. Applications of Sulfoxides to Asymmetric Synthesis of Biologically Active Compounds. *Chem. Rev.* **1995**, *95*, 1717–1760. [[CrossRef](#)]
30. Evans, D.A.; Andrews, G.C. Allylic sulfoxides. Useful intermediates in organic synthesis. *Acc. Chem. Res.* **1974**, *7*, 147–155. [[CrossRef](#)]
31. Fernández, I.; Khair, N. Recent Developments in the Synthesis and Utilization of Chiral Sulfoxides. *Chem. Rev.* **2003**, *103*, 3651–3706. [[CrossRef](#)] [[PubMed](#)]
32. Sipos, G.; Drinkel, E.E.; Dorta, R. The emergence of sulfoxides as efficient ligands in transition metal catalysis. *Chem. Soc. Rev.* **2015**, *44*, 3834–3860. [[CrossRef](#)] [[PubMed](#)]
33. Liang, J.J.; Gu, C.L.; Kacher, M.L.; Foote, C.S. Chemistry of singlet oxygen. 45. Mechanism of the photooxidation of sulfides. *J. Am. Chem. Soc.* **1983**, *105*, 4717–4721. [[CrossRef](#)]
34. Zou, Y.-Q.; Chen, J.-R.; Liu, X.-P.; Lu, L.-Q.; Davis, R.L.; Jørgensen, K.A.; Xiao, W.-J. Highly Efficient Aerobic Oxidative Hydroxylation of Arylboronic Acids: Photoredox Catalysis Using Visible Light. *Angew. Chem. Int. Ed.* **2012**, *51*, 784–788. [[CrossRef](#)] [[PubMed](#)]
35. Pitre, S.P.; McTiernan, C.D.; Ismaili, H.; Scaiano, J.C. Mechanistic Insights and Kinetic Analysis for the Oxidative Hydroxylation of Arylboronic Acids by Visible Light Photoredox Catalysis: A Metal-Free Alternative. *J. Am. Chem. Soc.* **2013**, *135*, 13286–13289. [[CrossRef](#)]
36. Klán, P.; Šolomek, T.; Bochet, C.G.; Blanc, A.; Givens, R.; Rubina, M.; Popik, V.; Kostikov, A.; Wirz, J. Photoremovable Protecting Groups in Chemistry and Biology: Reaction Mechanisms and Efficacy. *Chem. Rev.* **2013**, *113*, 119–191. [[CrossRef](#)]
37. Shao, Q.; Xing, B. Photoactive molecules for applications in molecular imaging and cell biology. *Chem. Soc. Rev.* **2010**, *39*, 2835–2846. [[CrossRef](#)]
38. Huang, L.; Zeng, L.; Chen, Y.; Yu, N.; Wang, L.; Huang, K.; Zhao, Y.; Han, G. Long wavelength single photon like driven photolysis via triplet triplet annihilation. *Nat. Commun.* **2021**, *12*, 122. [[CrossRef](#)]
39. Qiu, F.-Y.; Zhang, M.; Ji, R.; Du, F.-S.; Li, Z.-C. Oxidation-Responsive Polymer–Drug Conjugates with a Phenylboronic Ester Linker. *Macromol. Rapid Commun.* **2015**, *36*, 2012–2018. [[CrossRef](#)]
40. Peiró Cadahía, J.; Previtali, V.; Troelsen, N.S.; Clausen, M.H. Prodrug strategies for targeted therapy triggered by reactive oxygen species. *Med. Chem. Commun.* **2019**, *10*, 1531–1549. [[CrossRef](#)]
41. Mitsunaga, M.; Ogawa, M.; Kosaka, N.; Rosenblum, L.T.; Choyke, P.L.; Kobayashi, H. Cancer cell-selective in vivo near infrared photoimmunotherapy targeting specific membrane molecules. *Nat. Med.* **2011**, *17*, 1685–1691. [[CrossRef](#)] [[PubMed](#)]
42. DeForest, C.A.; Anseth, K.S. Cytocompatible click-based hydrogels with dynamically tunable properties through orthogonal photoconjugation and photocleavage reactions. *Nat. Chem.* **2011**, *3*, 925–931. [[CrossRef](#)] [[PubMed](#)]
43. Marinescu, L.G.; Pedersen, C.M.; Bols, M. Safe radical azidonation using polystyrene supported diazidoiodate(I). *Tetrahedron* **2005**, *61*, 123–127. [[CrossRef](#)]
44. Raza, F.; Park, J.H.; Lee, H.-R.; Kim, H.-I.; Jeon, S.-J.; Kim, J.-H. Visible-Light-Driven Oxidative Coupling Reactions of Amines by Photoactive WS₂ Nanosheets. *ACS Catal.* **2016**, *6*, 2754–2759. [[CrossRef](#)]
45. Patil, R.D.; Adimurthy, S. Copper-Catalyzed Aerobic Oxidation of Amines to Imines under Neat Conditions with Low Catalyst Loading. *Adv. Synth. Catal.* **2011**, *353*, 1695–1700. [[CrossRef](#)]
46. Su, C.; Tandiana, R.; Tian, B.; Sengupta, A.; Tang, W.; Su, J.; Loh, K.P. Visible-Light Photocatalysis of Aerobic Oxidation Reactions Using Carbazolic Conjugated Microporous Polymers. *ACS Catal.* **2016**, *6*, 3594–3599. [[CrossRef](#)]

47. Bradamante, S.; Colombo, S.; Pagani, G.A.; Roelens, S. The Reaction of Pyruvic Acid with Amines and Aminoesters Reexamined. Preliminary communication. *Helv. Chim. Acta* **1981**, *64*, 568–571. [[CrossRef](#)]
48. Sasamoto, N.; Dubs, C.; Hamashima, Y.; Sodeoka, M. Pd(II)-Catalyzed Asymmetric Addition of Malonates to Dihydroisoquinolines. *J. Am. Chem. Soc.* **2006**, *128*, 14010–14011. [[CrossRef](#)]
49. Wu, X.; Gorden, A.E.V. 2-Quinoxalinol Salen Copper Complexes for Oxidation of Aryl Methylenes. *Eur. J. Org. Chem.* **2009**, *2009*, 503–509. [[CrossRef](#)]
50. Sharma, A.; Sharma, N.; Kumar, R.; Sharma, U.K.; Sinha, A.K. Water-promoted cascade synthesis of α -arylaldehydes from arylalkenes using N-halosuccinimides: An avenue for asymmetric oxidation using Cinchona organocatalysis. *Chem. Commun.* **2009**, 5299–5301. [[CrossRef](#)]
51. Kasaya, Y.; Hoshi, K.; Terada, Y.; Nishida, A.; Shuto, S.; Arisawa, M. Aromatic Enamide/Ene Metathesis toward Substituted Indoles and Its Application to the Synthesis of Indomethacins. *Eur. J. Org. Chem.* **2009**, *2009*, 4606–4613. [[CrossRef](#)]